OPEN ACCESS

Vortex emissions from quantum turbulence generated by vibrating wire in superfluid ^{4}He at finite temperature

To cite this article: Y Wakasa *et al* 2014 *J. Phys.: Conf. Ser.* **568** 012027

View the article online for updates and enhancements.

Related content

- Generation and detection of vortex rings in superfluid ^{4}He at very low temperature
H Yano, A Nishijima, S Yamamoto et al.
- Analysis of motion of solid hydrogen tracer particles in oscillating superfluid flows
E Zemma, J Luzuriaga and S Babuin
- Turbulence in quantum fluids
Makoto Tsubota

Recent citations

- Vortex Emission from Quantum Turbulence Generated by Vibrating Wire in Superfluid $$^4\hbox {He}$$4He
H. Yano *et al*
- Anisotropic Formation of Quantum Turbulence Generated by a Vibrating Wire in Superfluid $${}^{4}\hbox {He}$$ 4 He
H. Yano *et al*

This content was downloaded from IP address 23.168.145.20 on 31/08/2021 at 15:05

Vortex emissions from quantum turbulence generated by vibrating wire in superfluid ^{4}He at finite temperature

Y Wakasa, S Oda, Y Chiba, K Obara, H Yano, O Ishikawa, and T Hata

Graduate School of Science, Osaka City University, Osaka 558-8585, Japan

E-mail: hideo@sci.osaka-cu.ac.jp

Abstract. An oscillating object immersed in superfluid helium generates quantum turbulence, emitting quantized vortices to its surroundings. We report vortex emissions in directions parallel and perpendicular to the oscillating motion of a thin wire used as a turbulence generator. Two vibrating wires are used to detect the vortex emissions. We use superfluid ^{4}He as a medium, with the temperature set to 1.25 K, at which a small amount of normal fluid component is present. In this setup, only vortex loops with sizes larger than a certain loop diameter $D = 42\ \mu$m can be detected. In the perpendicular direction, vortex loops are detected when the oscillation amplitude is comparable with D. In the parallel direction, however, no vortex loops are detected at the same amplitude, suggesting an anisotropic emission of vortex loops.

1. Introduction

Turbulent flow in superfluids has a simpler structure than classical turbulence in viscous fluids [1]. Since the circulation of superfluids is quantized, superfluid flows consist only of quantized vortices. These vortices carry the same quantized circulation κ and have very thin cores, e.g. the core radius of a superfluid ^{4}He vortex is $a_0 \sim 0.1$ nm. A disordered tangle of quantized vortices produces turbulence in superfluid flow, namely quantum turbulence. Quantum turbulence is a central issue in low-temperature physics [2].

In experiments, quantum turbulence can be produced by a vibrating obstacle immersed in superfluid helium, even at very low temperature [3, 4]. Since a quantized vortex cannot have an unconnected end in superfluid helium, a vortex line forms a loop or it ends at the superfluid boundary. If the boundary is moved, superfluid flows arise along the surface of the boundary, causing vortex lines remaining at the boundary to move. A strongly vibrating motion of an object stretches vortex lines attached to the object, producing vortex loops by reconnection between vortex lines. Some of the vortex loops move away from the oscillation path, and others collide with the object during the return motion, producing further vortex loops. Thus, a vortex tangle forms in the oscillation path and vortex loops are emitted from the vortex tangle.

The motions of vortices are described as being governed only by quantized circulations in superfluids at the zero temperature limit. A circular vortex loop, for instance, moves in a superfluid sea, propelled by quantized circulation with a velocity [5]

$$v = \frac{\kappa}{4\pi R}\left(\ln\frac{8R}{a_0} - \frac{1}{2}\right), \tag{1}$$

where R is the radius of the vortex loop. Despite the simplicity of the description, experimental studies on the motion of vortex loops are quite difficult because there are few methods for vortex observation.

Content from this work may be used under the terms of the Creative Commons Attribution 3.0 licence. Any further distribution of this work must maintain attribution to the author(s) and the title of the work, journal citation and DOI.
Published under licence by IOP Publishing Ltd

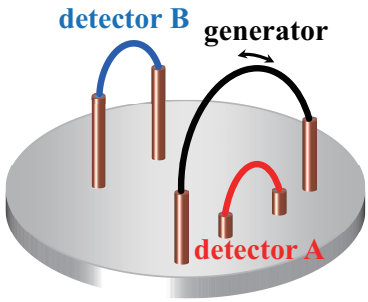

Figure 1. Schematic of vibrating wires. The detector wires are mounted around the generator wire. Detectors A and B are located in directions perpendicular and parallel, respectively, to the vibration direction of the generator indicated by the arrows. The distances between the generator and detectors A and B are 0.84 mm and 0.83 mm, respectively.

Visualization techniques for quantized vortices can trace vortex motions [6, 7], though these techniques have been limited to studies on quantized vortices at high temperatures. Also, tracer particles may affect the vortex motions.

Recently, the paths of vortices emitted from turbulence have been studied by using vibrating wires [8, 9]. A vortex-free vibrating wire, which cannot generate turbulence alone even at high vibrating velocities, is capable of detecting a vortex loop [4]. When a vortex loop collides with a vortex-free vibrating wire, the vibration of the wire is dissipated due to generation of turbulence. After the wire vibration has been stopped, the wire returns to the vortex-free state [10]. A set of two vibrating wires, a turbulence generator and a vortex detector, enables the study of the time-of-flight of a vortex emitted from the generator to the detector. In the present paper, we report vortex emissions in directions parallel and perpendicular to the vibrating directions of a generator, generated in superfluid ^{4}He at a finite temperature.

2. Experimental setup

To detect vortex flight paths, we mounted three vibrating wires made of NbTi wire with a diameter of ~2 μm in a copper chamber with a pin hole. Two detector wires, detector A and detector B, are located in directions perpendicular and parallel, respectively, to the vibration direction of a generator wire, as shown in Fig. 1. The distance between the apexes of the generator and detector A is tuned to be 0.84 mm, with the distance between the generator and detector B set to be almost the same at 0.83 mm. The bending shape of detector A is nearly identical to that of detector B. Although the wire arrangement is similar to a previous experimental design [11], the tuned distances enable us to study the direction distributions of vortex emissions from the generator more precisely. The resonance frequencies in vacuum at 4.2 K are 1145 Hz for the generator, 2906 Hz for detector A and 3282 Hz for detector B.

To study vortex emissions for large vortex loops, we performed time-of-flight measurements in superfluid ^{4}He at a temperature of 1.25 K. At a finite temperature, a normal fluid component arises from superfluid helium, dissipating superfluid vortices. Vortex loops shrink during flight and may therefore fade away. The flight distance l and the flight time τ until disappearance of a circular vortex loop with a radius R_0 are given by $l = R_0/\alpha$ and $\tau = R_0/2\alpha v_0$ [5], where α is the mutual friction coefficient between a normal fluid component and a vortex line, and v_0 is the velocity of a loop with radius R_0 given by Eq. (1). In the present setup, the detectors can detect emitted vortex loops with an initial diameter only above 42 μm, because smaller vortex loops may disappear shortly before reaching the detectors. The flight time of the fastest loop is estimated to be 0.08 s under this condition.

3. Results and discussion

3.1. Time-of-flight measurements for the perpendicular direction

Time-of-flight measurements were performed by similar methods to those used in previous studies [9, 11]. We measured the period between the start of turbulence generation by the generator and the detection of a vortex loop by the detector. The period, therefore, corresponds to the creation time of a

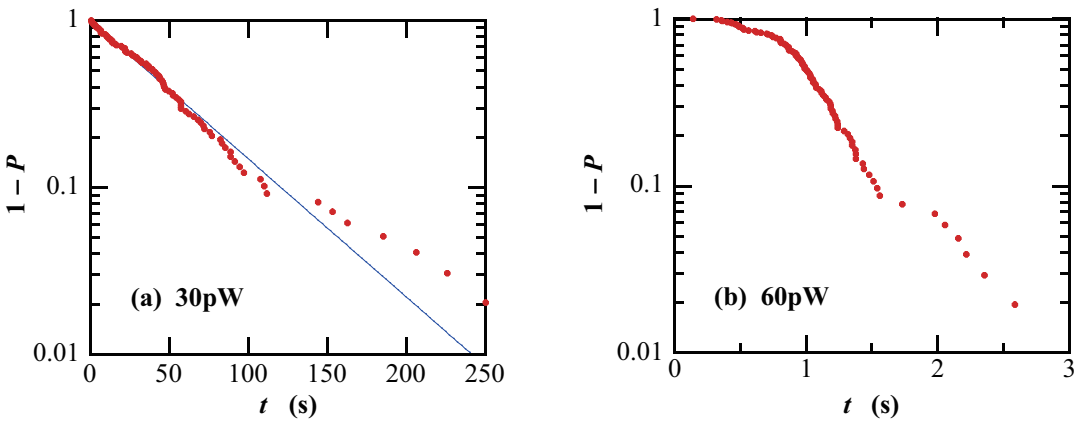

Figure 2. Distribution of vortices detected with detector A for generation powers of (a) 30 pW and (b) 60 pW. The probability P is the detection probability within a time period t. (a) The probability $1 - P$ for 30 pW follows the exponential function Eq. (2), shown by the solid line. (b) The detection periods for 60 pW are much shorter than those for 30 pW. The distribution, however, no longer shows a single exponential function (see text).

vortex loop plus the time of its flight from the generator to the detector. We measured periods repeatedly at a temperature of 1.25 K for a power of 30 pW injected in a turbulence region, and found that the observed periods were distributed widely from 0.4 s to 250 s for 100 measurements. The non-detection probability $1 - P$ is plotted as a function of time in Fig. 2(a), where P is the detection probability within a time window t. The data of the probability $1 - P$ are consistent with an exponential function

$$1 - P = \exp\left(-\frac{t - t_0}{t_1}\right), \tag{2}$$

shown as the solid line in Fig. 2(a), indicating that the vortex detection is a Poisson process. The fitting parameters t_0 and t_1 are estimated to be 0 s and 53 s, respectively. The parameter t_0 corresponds to the creation time plus the flight time of the fastest vortex loop [9]. As mentioned in the previous section, the flight time of the fastest vortex loop that can reach the detector is expected to be 0.08 s. The creation time of a vortex loop by the generator is expected to be less than 10 ms [9]. Therefore, the time t_0 is estimated to be almost zero in the present time range. The mean detection period corresponds to the fitting parameter t_1. Hence, the detector detects vortex loops at irregular intervals with a mean interval time of t_1. Since the detector can respond only to a reachable vortex loop, this result suggests that vortex loops are emitted randomly with respect to the emission direction. To study the emission rate of large vortex loops, we measured times-of-flight for different generation powers. For powers below 30 pW, we rarely detected vortex loops within a measurement time window of 500 s. For a power of 60 pW, however, the observed detection periods are much shorter than those for 30 pW, as shown in Fig. 2(b). The emission rate of large vortex loops appears to increase steeply with increasing generation power.

The data of the probability $1 - P$ for 60 pW do not fit to a single exponential function. The detection rate of vortex loops, proportional to the slope of the probability, increases at times above 0.8 s, in contrast to the 30 pW case. Increasing emission rates appear to affect the vortex emissions. It is plausible that emitted vortices reconnect between themselves at high densities, forming a tangle of vortices between the generator and the detector, as observed in the studies of superfluid ^{3}He-B [12]. Forming the tangle may reduce vortex loops reaching the detector. When a balance is achieved in the tangle, the detection rate increases, as the distribution above 0.8 s for the 60 pW case shown in Fig. 2(b).

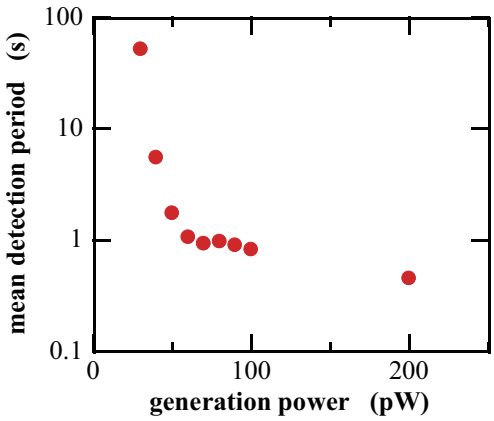

Figure 3. Mean detection period of detector A as a function of generation power. Below 50 pW, the distributions of detection period indicate a Poisson process. Above 60 pW, however, the distributions do not reveal a Poisson process. In the figure, therefore, we averaged the detection period for all powers instead of using time t_1 in Eq. (2) (see text).

3.2. Power dependence of vortex emission for the perpendicular direction

To study the emission rates, we measured the distributions of time-of-flight as a function of generation power. Below 50 pW, the data are consistent with a single exponential function, indicating a Poisson process. Above 60 pW, however, the distributions do not indicate a single exponential function. The mean detection period is equal to time t_1 of Eq. (2) in a Poisson process because the time t_0 is negligible, though we could not estimate t_1 for powers above 60 pW. Instead of using time t_1, we averaged the detection periods to estimate a mean detection period, as shown in Fig. 3. The mean detection period decreases steeply with decreasing power below 60 pW, though the value does not vary so much above 60 pW.

In the present setup, only vortex loops larger than 42 μm in diameter can reach the detector. The emission of such large vortex loops should relate to the geometry of the turbulent region. For a power of 60 pW, the generator wire produces a turbulent region of (wire thickness: 2.4 μm) $\times$ (wire length: 1.3 mm) $\times$ (vibrating peak-to-peak amplitude: 34 μm). Thus, the emitted vortex size, ~42 μm, is comparable with the vibrating amplitude. This result suggests that the vibrating wire stretches attached vortices, producing vortex loops comparable with its amplitude. The large vortex loops may propagate in the direction perpendicular to the vibration direction. In a previous paper [9], we found that a vibrating wire produces vortex loops equal to or smaller than 0.1 μm diameter. Consequently, a vibrating wire produces vortex loops with a diameter from 0.1 μm to a size comparable to its vibrating amplitude. Note that vortex loops with a larger size may not emit in this power range, because vortex loops have been rarely detected below 30 pW.

3.3. Vortex emission for the parallel direction

To study the direction distribution of vortex emissions, we measured times-of-flight for the direction parallel to the vibrating direction using detector B. Unlike in the perpendicular direction case, we did not detect vortices in a power range of the order of 10 pW to 100 pW. At 100 pW, we observed vortices within a time window of 500 s, though a few data points were still missing in the window. The detection periods are much longer than those for the perpendicular direction at the same power, indicating that large vortices are emitted anisotropically. The probability $1 - P$ of detection periods at 100 pW are well fitted to a single exponential function Eq. (2), as shown in Fig. 4, indicating a Poisson process. The fitting parameters t_0 and t_1 are estimated to be 0 s and 169 s, respectively.

This distribution suggests that vortices are emitted from the generator independently and randomly. This behavior is similar to that of the vortex emission for 30 pW in the perpendicular direction shown in Fig 2(a). The question remains, however, as to how the vibrating wire produces large vortex loops. In the parallel direction, the cross-section of a turbulent region for 100 pW has a geometry described by (wire thickness: 2.4 μm + wire bending: 0.9 μm) $\times$ (wire length: 1.3 mm). Thus, the largest vortex

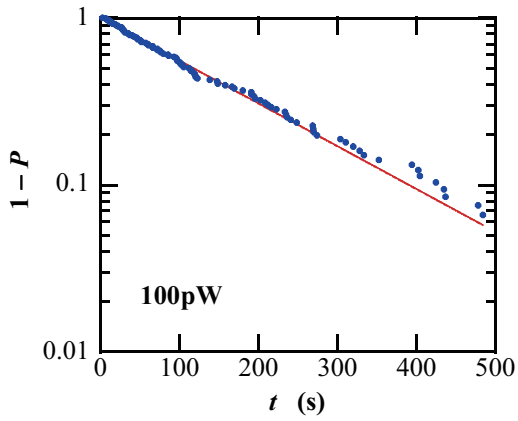

Figure 4. Distribution of vortices detected with detector B for a generation power of 100 pW. Here P is the detection probability within a time period t. The probability $1 - P$ is well fitted to the exponential function of Eq. (2), shown as the solid line.

loop produced by the generator is expected to be of the order of 1 μm, much smaller than the detected vortex loops. It is possible that large vortices may be emitted from tangles of vortices. As mentioned in the previous section, the distribution of the vortex emissions at 60 pW shown in Fig. 2(b) implies that a tangle of vortices may form around the generator. In a tangle of vortices, vortices reconnect between themselves, forming large vortex loops [12]. Therefore, it is plausible that large vortex loops may be emitted from tangles forming around the generator, though we cannot estimate the size of such tangles in this experiment.

In the present work, we observed anisotropic emissions of large vortex loops generated by a vibrating wire. In previous studies [13, 14], numerical simulations using a vibrating sphere also predict anisotropic emissions of vortex loops. Contrary to the present results, however, the emission rate of large vortex loops is higher in the direction parallel to the vibrating direction than that in the perpendicular direction. The emission rate of large vortex loops may be associated with the geometry of the vibrating object. A vibrating sphere produces a turbulence forming a column with a length equal to the vibrating amplitude and a diameter comparable with the sphere size. The turbulence produced by a vibrating wire may spread in a rather planar region defined by the vibrating amplitude and the wire length. Therefore, a vibrating wire can produce large vortex loops propagating in the perpendicular direction more easily. Further experimental and numerical studies are necessary to describe vortex emissions produced by a vibrating object.

4. Conclusions

We report the vortex emission of large vortex loops generated by a vibrating wire immersed in superfluid ^{4}He. Using vortex-free vibrating wires as a vortex detector, we measured times-of-flight in the directions perpendicular and parallel to the vibrating direction of the generator wire. In the perpendicular direction, the vibrating wire can produce vortex loops with a diameter comparable with the vibrating peak-to-peak amplitude. In the parallel direction, we also find the emission of such large vortex loops, though a higher generation power is required for large vortex loops to be detected. This anisotropy may be associated with the creation mechanism of large vortex loops.

Acknowledgments

The authors are very grateful to M. Tsubota and A. Nakatsuji for stimulating discussions. The research was supported by a Grant-in-Aid for Scientific Research (B) (Grant No. 23340108) from the Japan Society for the Promotion of Science.

References

[1] Vinen W F and Donnelly R J 2007 *Phys. Today* **60** No.4, 43

[2] Halperin W P and Tsubota M 2009 *Progress in Low Temperature Physics* vol 16 (Amsterdam: North-Holland)
[3] Fisher S N, Hale A J, Guénault A M and Pickett G R 2001 *Phys. Rev. Lett.* **86** 244
[4] Goto R, Fujiyama S, Yano H, Nago Y, Hashimoto N, Obara K, Ishikawa O, Tsubota M and Hata T 2008 *Phys. Rev. Lett.* **100** 045301
[5] Donnelly R J 1991 *Quantized Vortices in Helium II* (Cambridge, England: Cambridge University Press)
[6] Paoletti M S, Fiorito R B, Sreenivasan K R and Lathrop D P 2008 *J. Phys. Soc. Jpn.* **77** 111007
[7] Bewley G P and Sreenivasan K R 2009 *J. Low Temp. Phys.* **156** 84
[8] Kubo H, Nago Y, Nishijima A, Obara K, Yano H, Ishikawa O and Hata T 2013 *J. Low Temp. Phys.* **171** 466
[9] Nago Y, Nishijima A, Kubo H, Ogawa T, Obara K, Yano H, Ishikawa O and Hata T 2013 *Phys. Rev. B* **87** 024511
[10] Yano H, Nago Y, Goto R, Obara K, Ishikawa O and Hata T 2010 *Phys. Rev. B* **81** 220507(R)
[11] Oda S, Wakasa Y, Kubo H, Obara K, Yano H, Ishikawa O and Hata T 2014 *J. Low Temp. Phys.* **175** 317
[12] Fujiyama S, Mitani A, Tsubota M, Bradley D I, Fisher S N, Guénault A M, Haley R P, Pickett G R and Tsepelin V 2010 *Phys. Rev. B* **81** 180512
[13] Nakatsuji A, Tsubota M and Yano H 2013 *J. Low Temp. Phys.* **171** 519
[14] Nakatsuji A, Tsubota M and Yano H 2014 *Phys. Rev. B* **89** 174520